Postprint of: Ryl J., Wysocka J., Darowicki K., Determination of causes of accelerated local corrosion of austenitic steels in water supply systems, CONSTRUCTION AND BUILDING MATERIALS, Vol. 64 (2014), pp. 246-252, DOI: 10.1016/j.conbuildmat.2014.04.058

Determination of causes of accelerated local corrosion of austenitic steels in water supply systems

J. Ryl[a,*], J. Wysocka[a], K. Darowicki[a]

[a]Department of Electrochemistry, Corrosion and Materials Engineering,

Gdansk University of Technology, Narutowicza 11/12, 80-952 Gdansk, POLAND

Corresponding author: jacek.ryl@pg.gda.pl, tel./fax +48 583471092

Abstract

This paper concerns an inspection of a water supply system, made of AISI 304 steel, which showed signs of local corrosion at the weld. Such corrosion caused material perforation after very short periods of operation. It was revealed that steel was sensitized during the welding process. It was also proven that chromium micro-segregation occurred in the alloy leading to galvanic cell formation which initialized the process of pitting corrosion. This paper is a study of corrosion attack types due to negligence during and after the process of welding of the system.

Key words: pitting corrosion, intergranular attack, weld decay, stainless steel

1. Introduction

Austenitic steel such as AISI 304 and AISI 316 are most often used as elements of industrial structures operated in conditions characterised by higher corrosion aggressiveness. Such steels are expected to be very resistant, in particular in water with a low content of chloride ions. For many water supply systems, however, accelerated degradation due to corrosive factors can be observed. Such resistance is ensured by a thin passive layer on the steel surface. Degradation of the passive layer, which is usually caused by external factors, can result in enhanced susceptibility of steel to local corrosion.

A key factor that causes the occurrence of local corrosion is the presence of chloride ions. There are many theories pertaining to their influence on pitting corrosion [1-3]. Most of them suggest adsorption of Cl^- ions on the layer surface which later becomes oxide-depleted. Safe concentrations of chloride ions that do not cause pitting corrosion of austenitic steels are conditioned by the grade of steel as well as many environmental factors. The Langelier Saturation Index (LSI) is a popular method of evaluating water quality data to determine if the water has a tendency to form chemical scale. In order to use this index, the following laboratory analyses are needed: pH, conductivity, total dissolved solids, alkalinity, and total hardness.

Local corrosion can be often observed along sections of pipelines with a very limited flow and in standing water, e.g. in fire protection or potable water systems. In such cases, crevice corrosion is particularly hazardous. This type of corrosion is also hazardous for connections of elements [4] or in areas where organic coating is loosening. Further, anaerobic areas also contribute to corrosion due to microbiological activity where e.g. sulphate-reducing bacteria (SRB) and/or iron-oxidizing bacteria (IOB) can grow [6,7]. It is believed that even up to 10% of all corrosion damage can be caused by such microbiological activity.

Buried elements of steel structures, arranged in urbanized areas, are even more exposed to sources of chloride ions from salt used by road services to sprinkle roads. Conducted research has proven that even up to 50% of salt penetrates locally to surface waters [8], and the content of chloride ions can reach even up to 2700 mg/l [9].

Due to high temperatures associated with the welding process, where such temperatures can cause structural changes in steel, the heat-affected zone at the weld is often the area where accelerated local corrosion occurs. After welding, it is important that the surface that could be in contact with water has a homogeneous composition. Any crevices formed during the process should also be removed. Due to steel sensitization during the welding process, areas of higher susceptibility to intergranular corrosion are often created. Such corrosion is often associated with pitting corrosion resulting from concentration cells in the alloy created due to uneven distribution of chromium. Once a pit has been created, it acts as an anode depolarized by an extensive cathodic area around the pit, and causes intensive degradation. Most often pitting occurs in heterogeneous materials. This complex corrosion process in the heat-affected zone, causing material loss along the weld, is referred to as weld decay [10-12]. Degradation due to local corrosion can be much faster than could be expected for the construction materials used and corrosive aggressiveness of the environment.

In addition, a combination of corrosive and mechanical factors such as erosion or cavitation erosion-corrosion can have a synergy effect that usually enhances the rate of material degradation. This type of hazard occurs particularly in systems with a turbulent flow of liquid [13-16].

This paper is a case study relating to the causes of local corrosion in the water supply system.

2. Experimental

The structure being the subject of this investigation is an element of a water supply system, described in the next chapter. Corrosion causes pipeline perforation resulting in the appearance of corrosion products on the outer walls. This effect can be observed in the vicinity of welded joints. For experimental purposes, a section of the pipeline, including the weld and the parent material at a distance of around 5 cm from the welded joint, was sampled. The inner diameter of the pipe under examination was equal to 30 cm and its thickness was 0.4 cm. Weld bead width was around 1.2 cm while effect of welding in the form of discoloration was visible up to 1.5 cm from the weld bead. Also for the purpose of the experiment, the film of corrosion products on the inner side, was etched in a mixture of organic acids and corrosion inhibitors used for cleaning chromium-nickel steel.

Within the testing procedure, the grade of the steel subjected to testing was identified by optical emission spectrometry with glow discharge and with the use of spectroscope LECO GDS850A. In addition, physical and chemical parameters of water flowing through the pipeline were analysed to determine the LSI index. Analytical tests of water were carried out by means of the colorimetric method with the use of a Palintest Photometer 5000 system offering an instrumental method of a wide range of water tests. Determination of dry residue was carried out in accordance with standard PN-EN 12880:2004. Other parameters determined included: pH – with a microcomputer meter CP-551, conductivity – with a microcomputer conductometer CC-315, oxygen – with an oxygen meter CO-411.

An analysis by means of the cyclic polarisation method carried out within this study was conducted with the use of a three-electrode system where the tested pipeline section was the working electrode. Its surface area was 2 cm^2. A saturated calomel electrode (SCE) was used as a reference electrode, whereas platinum gauze served as the counter electrode. A 150 ml solution of

water transported in the pipeline and polarisation rate of 1 mV/s were applied. For the purpose of tests, a potentiostat manufactured by GAMRY International was used.

Topography analysis of sample was carried out on Hitachi S-3400N scanning electron microscope with a tungsten source and variable chamber pressure (VP-SEM). Pictures were taken in the secondary electrons mode (SE), under 20kV accelerating voltage and 10 mm working distance, proven as the optimal conditions. The microscope was equipped with an energy-dispersive spectroscope EDX, manufactured by ThermoScientific, as an attachment.

3. Results and discussion

3.1. Inspection of the water supply system

Various areas of the system were inspected, corrosion had the same character and origin for every element of the pipeline. Most often corrosion occurred just at the weld or in its vicinity, not further than 3 cm away from the weld. Washed-away corrosion products flow slowly out of the perforation areas. The photos in Fig. 1 illustrate corrosion damage of different pipelines within the water supply system, in particular: pumping station (Fig. 1a-b), rinsing water system (Fig. 1c), water filtration system (Fig. 1d). In addition, it was found that there were attempts to remove perforation due to corrosion by pad welding (Fig. 1d).

A preliminary visual inspection of the pipeline showed that compacted corrosion products were accumulated on its inner side (Fig. 2a-b). The areas correspond to the spots where stains on the outer side were located. Moreover, in the vicinity of the weld, the entire area was covered with a thin layer of rust. Its presence indicates that there was no protective passive layer on the steel surface and iron corrosion occurred as a result. Once the section was cleaned, dark line located about 1 cm from the

weld was found (pointed out with arrows on Fig. 2c). In this area, macroscopic pits were revealed under the agglomeration of corrosion products (Fig. 2d).

An internal inspection of the pipeline carried out upon collecting the specimen showed that there were no such corrosion products further away from the weld. The photo in Fig. 3 reveals the same dark line within a direct distance from the weld. Its presence indicates an area of a thick layer of chromium oxides; the layer was formed as a result overheating during the welding process [17].

3.2. Water analysis

The pipeline is used for transporting untreated water. Its detailed composition as well as characteristic physical and chemical parameters are summarized in Table 1.

Based on the list of the above parameters the Langelier Saturation Index (LSI) was determined. The tested water is characterized by considerable hardness, a high total content of chlorides and sulphates, average conductivity, and a low oxygen content. There is no tendency for deposits for cold or hot water (at a temperature of 55 °C). Conditions for the formation of the passive layer are met, whereas there is no tendency to form deposits limiting the risk of crevice corrosion. There is a higher risk due to contact corrosion. In particular, a high content of chlorides significantly increases susceptibility to pitting corrosion in the aforementioned environment.

3.3. Local corrosion of steel

In most cases, the weld constitutes an area which is considerably different from the parent material in terms of its micro-structure, and even its chemical composition. These differences can contribute to the formation of galvanic cells with various stationary potentials, and as a result, to

corrosion of the area in the vicinity of the weld. In the very weld there are also micro-cells formed as a result of micro-structure segregation which occurs during solidification. If material used for welding is different from the parent material, such a situation can result in a considerable difference in potentials, and consequently, individual areas at the weld become more active and prone to corrosion. For instance, if welding AISI type 304 steel with metal which is rich in chromium and nickel, high differences in concentration of these elements influence weld corrosivity.

An analysis of chromium, nickel, molybdenum and carbon which was performed in bulk of the material to identify the steel grade showed that this is austenitic steel, grade AISI 304. Both the chromium and nickel content fall within lower allowable limits set out in the standard (Table 2). A spectrophotometry analysis was carried out for the parent material at a distance of about 5 cm from the weld and at the weld joint. A comparison of composition at both points was aimed at determining the validity of selecting the weld metal for the purpose of pipeline welding.

Although the materials applied for welding purposes were selected properly, the choice was not optimal. Steel AISI type 304 should be welded with the use of steel with molybdenum within the range of 2-2.5% or with 2-3% more chromium. Based on the samples of the weld and the parent material collected for the test, a higher content of chromium in the weld and a slightly higher content of molybdenum can be observed. However, the content of the latter element is too low to regard it as welding with the use of AISI 316 steel.

An analysis of chemical composition of the sample in a direct vicinity of the weld, within oxidized area (as presented in Fig. 2c) , was carried out. The oxidized area width is up to 1 cm. Fig. 4 presents relative information on the surface gradient of chromium and oxygen concentration with the use of Energy Dispersive X-ray Spectrometry (EDX). The obtained results prove an increased content of chromium and oxygen within the oxidized area, as compared to the weld and the area of the parent material (on the outer sides of the diagram). However, the results obtained with the help

of the EDX method with reference to thin films should be regarded as demonstrative because the area subject to the analysis is greater than the thickness of the passive layer; therefore just a part of the signal corresponds to it, whereas the rest corresponds to the bulk of the material. Still, the diagrams illustrate changes in the analysed parameters accurately.

The welding process, in particular in the case of low-quality gas arc welding, can lead to considerable differences in passive film thickness. If the alloy steel is not protected against atmospheric air properly or if it is subjected to severe grinding process, a thick passive layer is created on steel surface. Such a deformed layer of chromium oxides does not have barrier properties against a corrosion-aggressive medium, and as such, it does not provide proper protection against local corrosion. The chromium-depleted metal under such a layer contributes to the formation of concentration cells and can be the cause of pitting corrosion within and in the proximity of the heat-affected zone. When austenitic steel is kept at high temperatures when the process of sensitization occurs, areas depleted of chromium are also very susceptible to intergranular corrosion. It is very important that both the degraded layer of chromium oxides and the depleted area under the layer are removed mechanically (by grinding with small grit-size abrasive paper) or chemically (by a mixture of nitric acid and hydrofluoric acid). Once cleaned, the surface should be subject to passivation. However, this process was not carried out.

While welding high-alloy steels, areas with a higher risk of local corrosion are often created. In order to determine steel susceptibility to intergranular corrosion, metallographic pictures were taken at the specimen cross-section for the area of the parent material and underneath the oxidised layer. Earlier, the samples were subjected to chemical etching with Adler's reagent in order to uncover the metallographic structure of the steel. Pictures taken by a metallurgical microscope are presented in Fig. 5. Welded joint area, presented on Fig. 5a, is of completely different structure than heat-affected zone or base metal (Fig. 5b-c), wherein the sample has an austenitic structure. In the area beneath

oxidised layer, etching points at grain boundaries indicating the occurrence of intergranular corrosion are well visible. Also, the grains within this area are more coarse. Such degradation is not visible within the parent material. Susceptibility of the oxidised area to intergranular corrosion proves the presence of broad heat-affected zone underneath it.

In addition, a Strauss test was carried out, i.e. a test carried out with the use of 18% sulphuric acid and copper(II) sulphate [18]. The Strauss test revealed that steel in the section of the pipeline is prone to intergranular corrosion both in the broad area underneath oxides and heat-affected zone as well as in the parent material. Steel susceptibility to intergranular corrosion is proven by lost resonant sound of metal when hit as well as the photos taken by the scanning electron microscope (SEM) presented in Fig. 6.

Corrosion attack typical of intergranular corrosion is visible both in the heat-affected zone in a direct vicinity of the weld and further away in the parent material, up to a few centimetres from the weld. Intergranular attack revealed the structure within HAZ to be of smaller grain sizes. With the distance from the weld, the depth of the intergranular attack raise as well as the grain sizes. The cracks are most dominant in the oxidized area, around 1 cm from the weld, where susceptibility to intergranular corrosion increased considerably due to sensitization. The weld face was the only area where intergranular corrosion was not found. This area also maintained its resonant property. Additionally, SEM image taken in the oxidized area (Fig. 7) show joint intergranular and pitting corrosion, as is in case of the weld decay.

Sensitization is a parameter depending on, above all, the temperature, time of heat treatment, and carbon content in steel. If cooling after heat treatment takes place appropriately fast and the carbon content is appropriately low, the phenomenon of steel sensitization does not occur. If cooling from 900 to 400 ^{o}C takes place within about 1 minute, it will ensure resistance to intergranular corrosion of steel having up to 0.08% of carbon. A similar procedure that lasts about 1 hour

necessitates that carbon content is reduced to 0.03% [19]. For very slow cooling, the sensitization area is more extensive because the formation of chromium carbides takes place at higher temperatures.

Fig. 8 presents a SEM micrograph of an area surrounding corrosion pits connected in a crack. Similar to Fig. 7, the picture was taken within the oxidized area. The image was overlaid with a local analysis of chromium in steel, carried out by the EDX technique.

A chemical analysis proved micro-segregation of chromium in the vicinity of the corrosion pit and confirmed that steel sensitization occurred. The chromium content along a section of about 100 μm ranges from about 4.5% to even 40%. Such considerable local variations of the chemical element lead to the creation of concentration cells that intensify the rate of local corrosion, whereas a locally lower content of chromium below 12% results in disappearance of the passive layer, and as such protective properties of high-alloy steel as well. Even if chromium content is not below 12%, local galvanic cells can form which can lead to pitting. Such corrosion is caused by degradation of the thin passive layer that protects the metal [20,21].

Chromium micro-segregation that leads to local degradation of the passive layer additionally contributes to a rapid increase in the susceptibility to pitting corrosion [22]. The method of polarisation curves was applied to determine susceptibility of the pipeline section element to pitting corrosion within the area of the oxidised blue passive layer and the parent material. Water flowing through the pipeline served as the medium. Polarisation curves are presented below (Fig. 8).

The polarisation curves indicate steel susceptibility to pitting corrosion in both cases (Fig. 9); a hysteresis loop is visible. Pitting potential for both cases is about +0.5 V with reference to the silver chloride electrode. Re-passivation potential in the area of the parent material is 0.1 V and is higher than for the oxidised film area by about 0.2 V. In addition, the polarisation curve plotted for the area in the vicinity of the weld is characterised by rapid fluctuations in the current within the range before

the pitting potential. It is typical of steel undergoing pitting corrosion and is characteristics of the creation of metastable pits on the sample surface. The analysis of water revealed a high content of chlorides. As shown by the polarisation curves, the presence of chlorides causes pitting corrosion also in the area of steel parent material. Therefore, steel AISI type 304 is not an optimal choice in terms of corrosion resistance, and in particular, in the case of additional factors such as heat treatment after welding, it can be susceptible to local corrosion to a significant extent.

An inspection of magnetic properties revealed that the pipeline attracts a magnet at the weld and in its direct vicinity. No ferromagnetic properties were noticed on the pipeline surface further from the weld. As the pipe material attracts a magnet, it indicates structural changes that occurred in the material due to heat treatment, i.e. welding. This is additionally supported by metallographic image presented on Figure 5a. The corrosion behaviour of stainless steel weld deposits and castings is measurably different depending on whether the stainless steel has a micro-structure generated with primary ferrite or primary austenite. An optimum condition can be attained for ferrite contents between 3 and 8 %.wt in the weld deposit. When steel becomes sensitized at high temperatures during welding, ferrite σ can be formed [23-25].

It is possible to control the degree of sensitization of high-alloy steels by means of e.g. additional hardening after welding to dissolve chromium at grain boundaries again. Such a procedure usually cannot be applied at welded structures. Application of low carbon equivalents of steel, e.g. 304L instead of 304 or 316L instead of 316, provides good results by extending the time required for steel sensitization to occur. Steels containing titanium or niobium due to higher affinity of such elements to carbon are also used [26]. It is preferred that their carbides are formed, as they will prevent chromium depletion in grains. Another solution to avoid intergranular corrosion is to use alloys with a very high concentration of chromium so that local concentration cannot fall to 12%.

4. Conclusions

The pipeline corroded as a result of the so-called weld decay that caused pits perforating through the material. The location of pitting corrosion is not accidental and happens to be within the broad heat-affected zone, that reach up to few centimetres. At that distance, layer enriched with chromium oxides is present on the surface. Higher susceptibility to corrosion results from an improper steel welding process in combination with the presence of an aggressive environmental factor. This layer has to be removed chemically or mechanically just after welding, including the deeper area where the content of chromium is depleted.

The metallographic analysis revealed the presence of intergranular corrosion in the heat-affected zone. This type of corrosion occurs due to steel overheating (referred to as sensitization). Due to the segregation of chemical elements, corrosion is also associated with pitting corrosion that leads directly to pipeline perforation. Local segregation of chemical elements was confirmed by a point analysis of corrosive potential and the EDX method.

References:

[1] Lin LF, Chao CY, Macdonald DD. A point defect model for anodic passive films: II. Chemical breakdown and pit initiation. J Electrochem Soc 1981; 128: 1194 – 1198.

[2] Leckie HP, Uhlig HH. Environmental factors affecting the critical potential for pitting in 18 – 8 stainless steel. J Electrochem Soc 1966; 113: 1262 – 1267.

[3] Hoar TP. The production and breakdown of the passivity of metals. Corros Sci 1967; 7: 341 – 355.

[4] Ahmed TM, Alfantazi A, Budac J, Freeman G. Failure analysis of 316L stainless steel tubing of the high – pressure still condenser. Eng Fail Anal 2009; 16: 1432 – 1441.

[5] Song FM. A mathematical model developed to predict the chemistry and corrosion rate in a crevice of variable gap. Electrochim Acta 2011; 56: 6789 – 6803.

[6] Rao TS, Sairam TN, Viswanathan B, Nair KVK. Carbon steel corrosion by iron oxidising and sulphate reducing bacteria in a freshwater cooling system. Corros Sci 2000; 42: 1417 – 1431.

[7] Dinh HT, Kuever J, Mußmann M, Hassel AW, Stratmann M, Widdel F. Iron corrosion by novel anaerobic microorganism. Nature 2004; 427: 829 – 832.

[8] McConnell HH, Lewis J. Add salt to taste. Environment 1972; 14: 38 – 48.

[9] Bester ML, Frind EO, Molson JW, Rudolph DL. Numerical investigation of road salt impact on an urban well field. Ground Water 2006; 44: 165 – 175.

[10] Gooch TG, Willingham DC. Weld decay in AISI 304 stainless steel. Met Const Brit Weld J 1971; 3: 366.

[11] Kokawa H. Weld decay – resistant austenitic stainless steel by grain boundary engineering. J Mater Sci 2005; 40: 927 – 932.

[12] Song M, Guan KS. Failure analysis of a weld – decayed austenitic stainless steel. Eng Fail Anal 2011; 18: 1613 – 1618.

[13] Tan KS, Wharton JA, Wood RJK. Solid particle erosion – corrosion behavior of a novel HVOF nickel aluminium bronze coating for marine applications – correlation between mass loss and electrochemical measurements. Wear 2005; 258: 629 – 640.

[14] Kwok CT, Cheng FT, Man HC. Synergistic effect of cavitation erosion and corrosion of various engineering alloys in 3.5% NaCl solution. Mat Sci Eng 2000; A290: 145 – 154.

[15] Ryl J, Darowicki K. Impedance monitoring of carbon steel cavitation erosion under the influence of corrosive factors. J Electrochem Soc 2008; 155: P44 – P49.

[16] Klenowicz Z, Darowicki K, Krakowiak S, Krakowiak A. Corrosion – erosion damage of heat exchanger tubes by desalted crude oil flowing at shell side. Mater Corros 2003; 54: 181 – 187.

[17] Raman RKS, Gnanamoorthy JB. Oxidation behavior of weld metal, HAZ and base – metal regions in weldments of Cr-Mo Steels. Weld J 1995; 74: S133 – S139.

[18] ASTM A262-10 Standard practices for detecting susceptibility to intergranular attack in austenitic stainless steels.

[19] Davidson RM, DeBold T, Johnson MJ. Metals Handbook Vol 13, 9th ed.: ASM International; 1987.

[20] Orlikowski J, Darowicki K, Arutunow A, Jurczak W. The effect of strain rate on the passive layer cracking of 304L stainless steel in chloride solutions based on the differential analysis of electrochemical parameters obtained by means of DEIS. J Electroanal Chem 2005; 576: 277 – 285.

[21] Darowicki K, Orlikowski J, Arutunow A. Detection of stress corrosion cracking dynamics by dynamic electrochemical impedance spectroscopy. Corros Eng Sci Tech 2004; 39: 255 – 260.

[22] ASTM G46-76 Recommended practice for evaluation of pitting corrosion.

[23] Wahid A, Olson DL, Matlo DK. Corrosion of Weldments. ASM Handbook Vol 6: Welding, Brazing, and Soldering: ASM International; 1993.

[24] Backman A, Lundqvist B. Properties of a fully austenitic stainless steel weld metal for severe corrosion environments. Weld J 1977; 56: 23s – 28s.

[25] Menendez H, Devine TM. The influence of microstructure on the sensitization behavior of duplex stainless steel welds. Corrosion 1990; 46: 410 – 418.

[26] Čihal V. Intergranular corrosion of steels and alloys. Elsevier Science Publishers: BV; 1984.

Tables and Figures

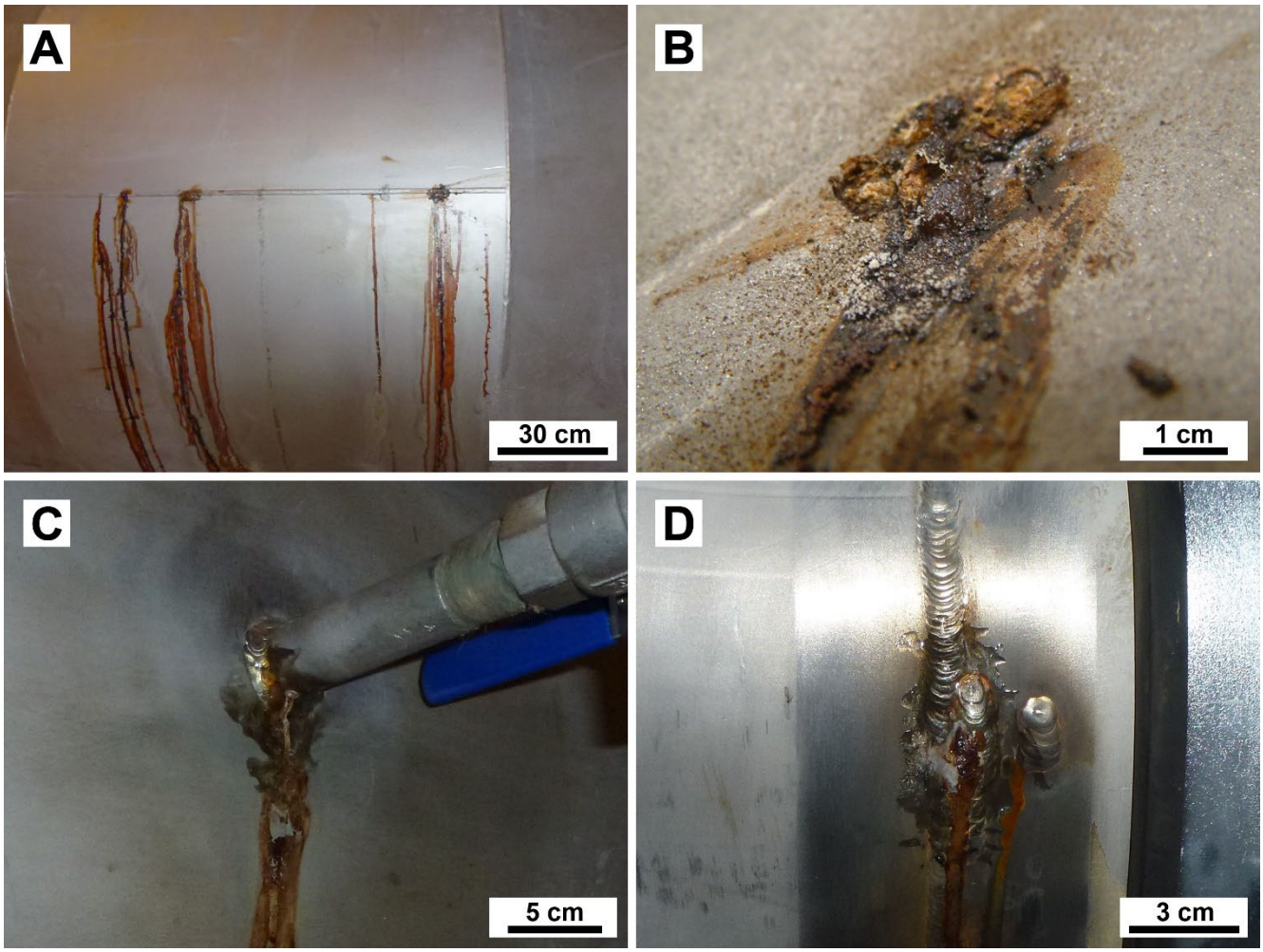

Figure 1 – Inspection of pipeline system, at: a,b) pumping station pipeline, c) rinsing water system pipeline, d) water filtration system pipeline.

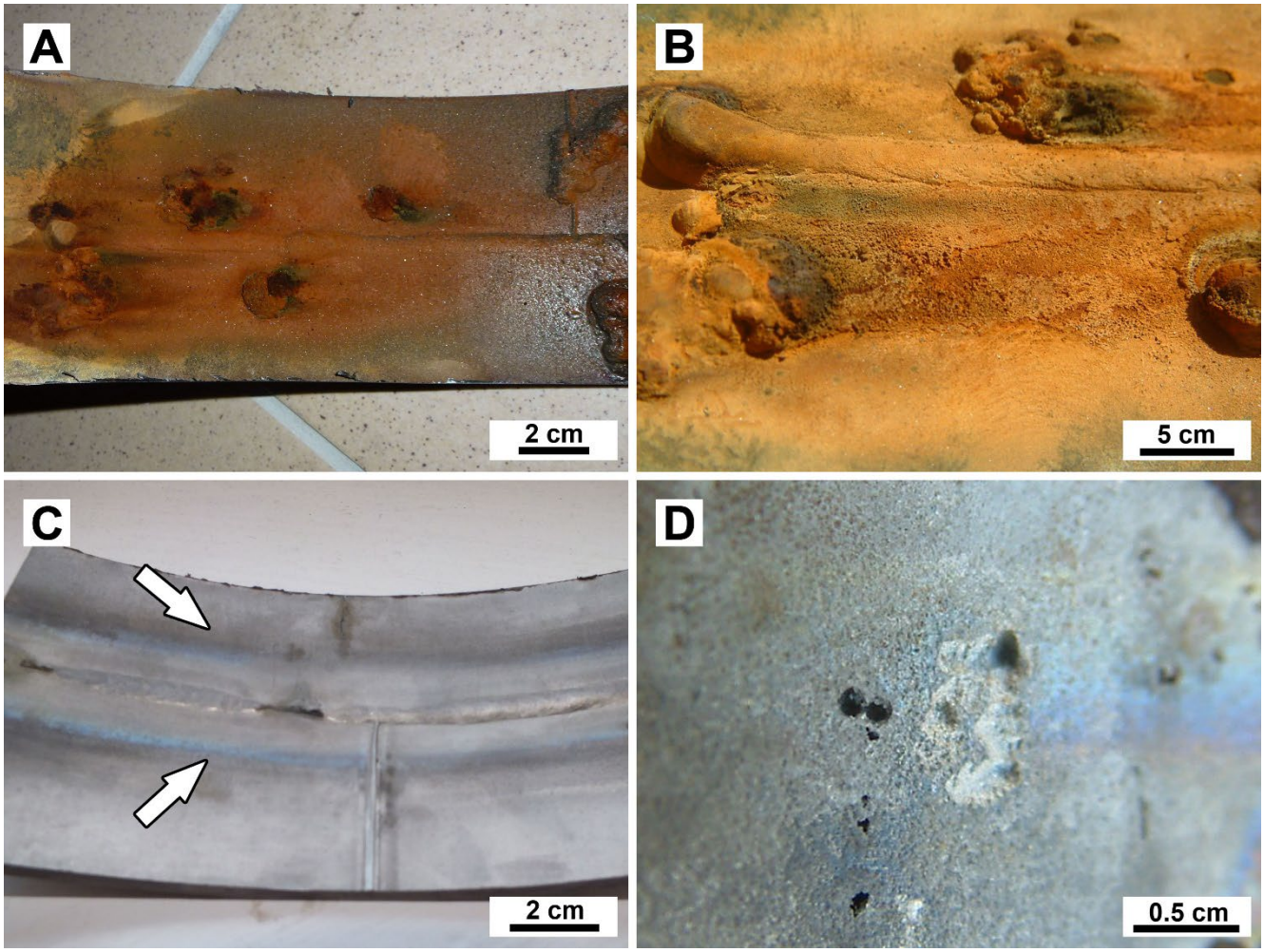

Figure 2 – Pipeline element taken for further analysis. a) specimen, b) a view of corrosion products on the inner side, c) the sample after immersing in inhibitors, d) corrosion pits

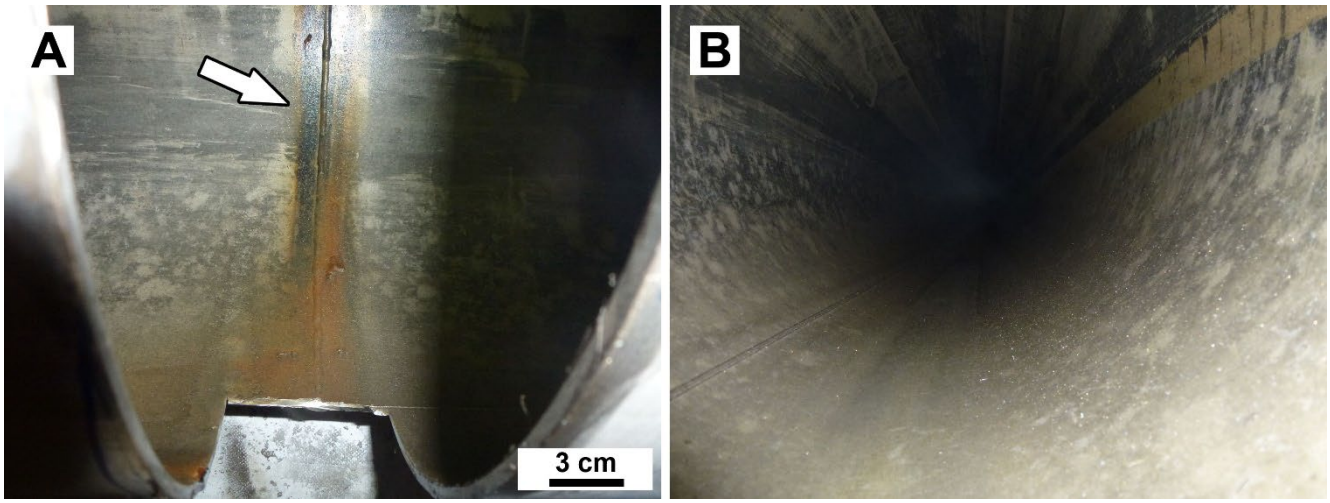

Figure 3. – A photo taken inside the pipeline at the specimen collection site.

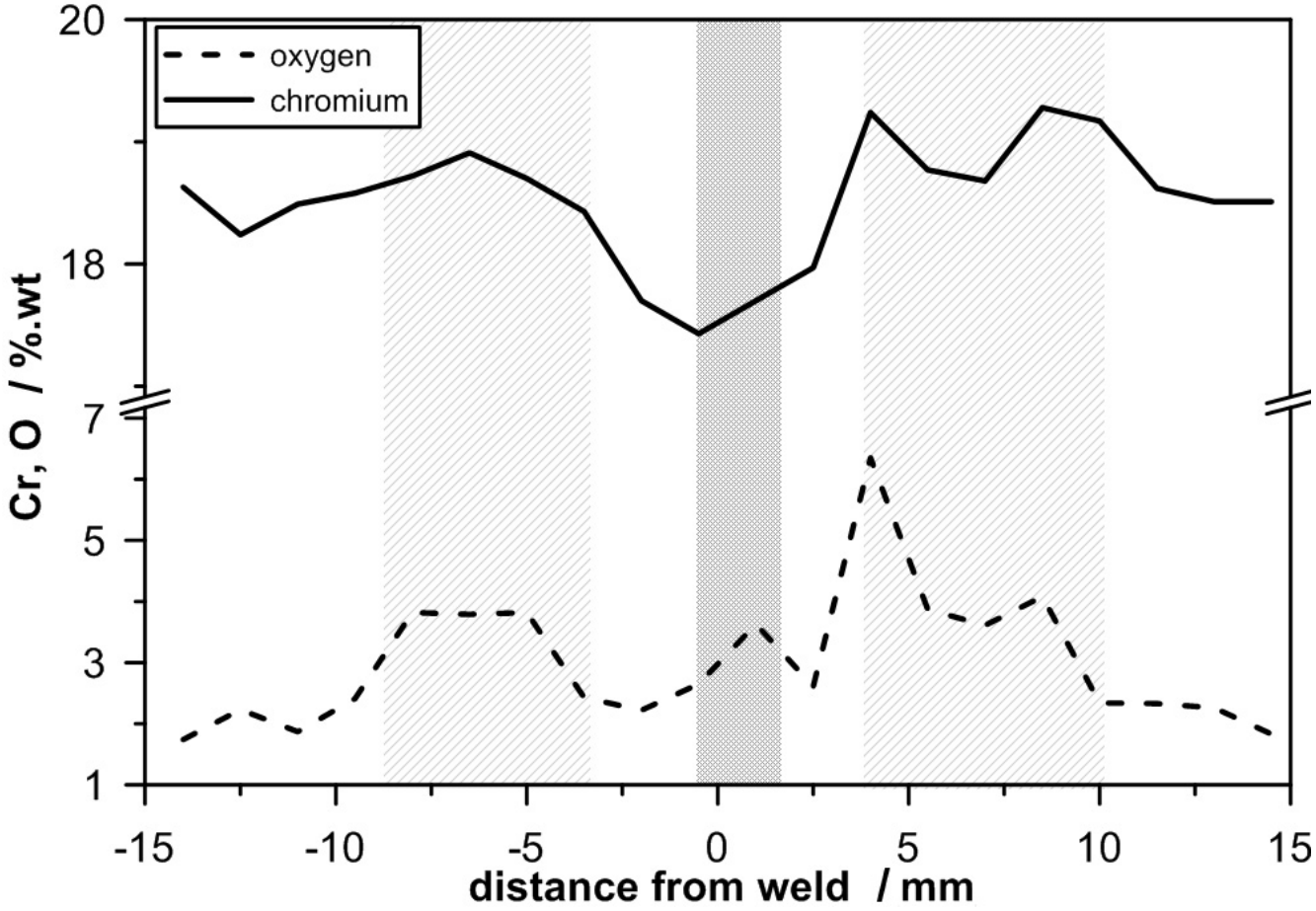

Figure 4 – Results of the EDX analysis concerning the content of chromium and oxide on the inner surface of the pipeline section. The shaded area corresponds respectively to (▒) the weld and (▨) the blue layer of chromium oxides.

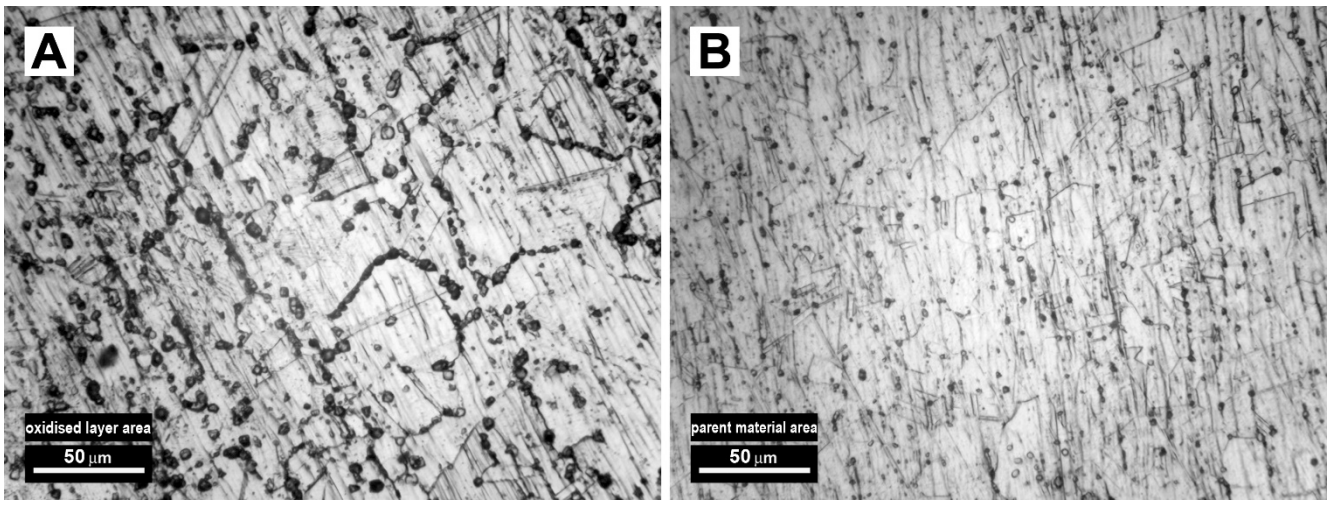

Figure 5 – Pictures of steel cross-sections taken by a metallurgical microscope: a) weld and heat-affected zone (magnification x100), b) heat-affected zone within the oxidized layer area (magnification x400), c) parent material (magnification x400).

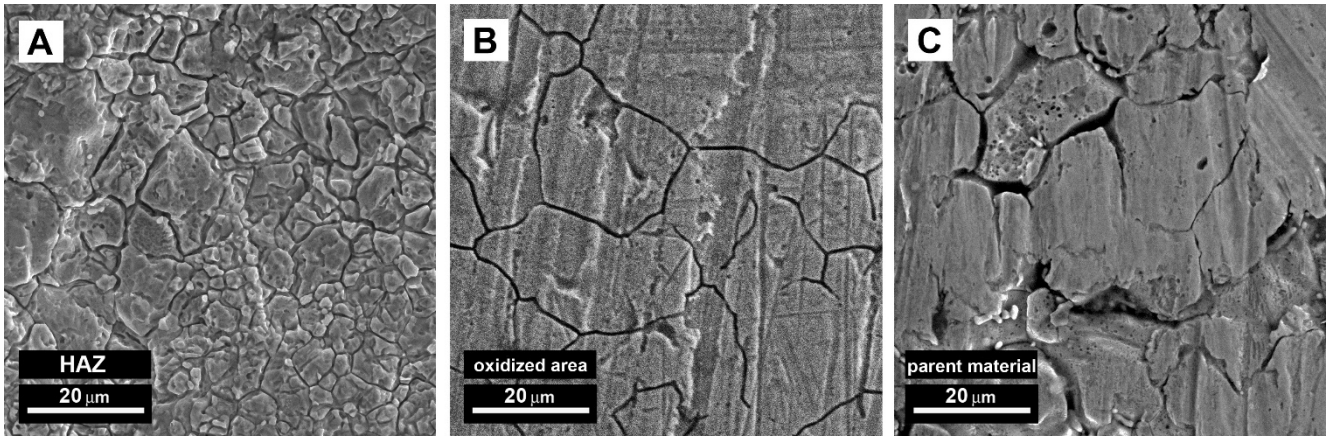

Figure 6 – SEM micrographs taken after Strauss test: a) heat-affected zone b) area of the parent material. Magnification x1000

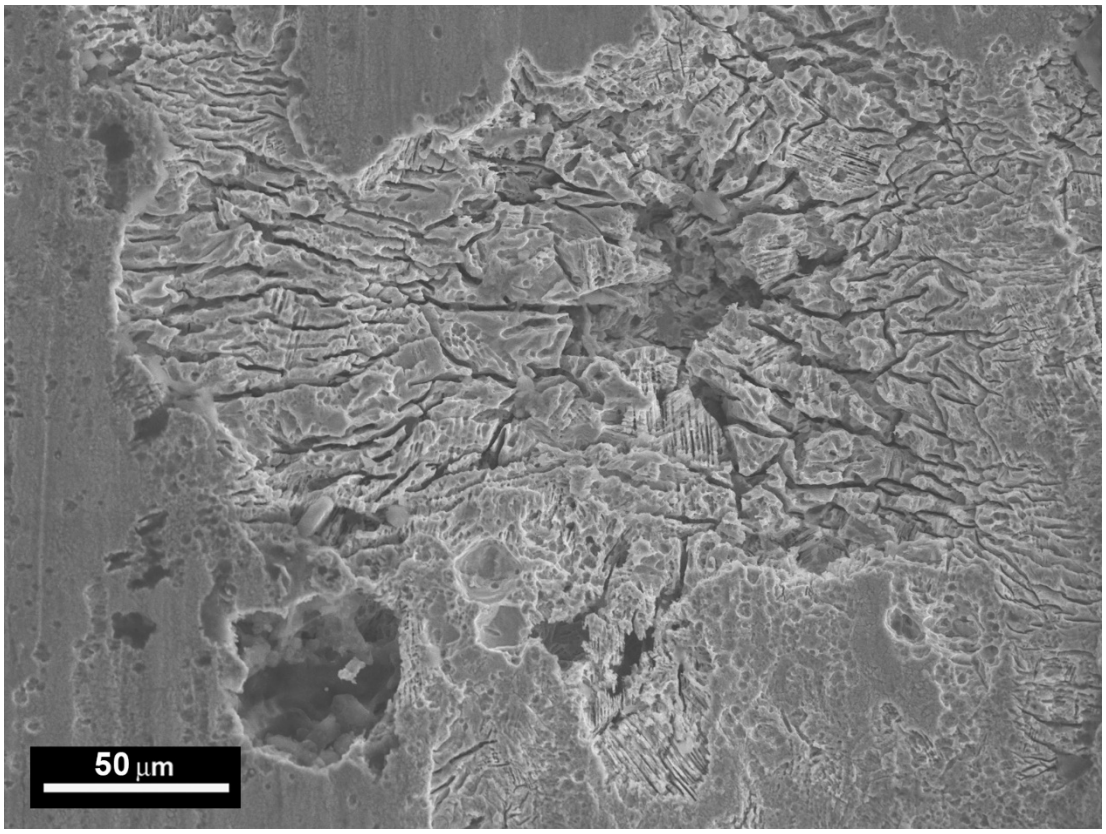

Figure 7 – SEM micrographs of a join pitting and intergranular corrosion within the heat-affected zone, proving weld decay presence. Picture taken after Strauss test. Magnification x500.

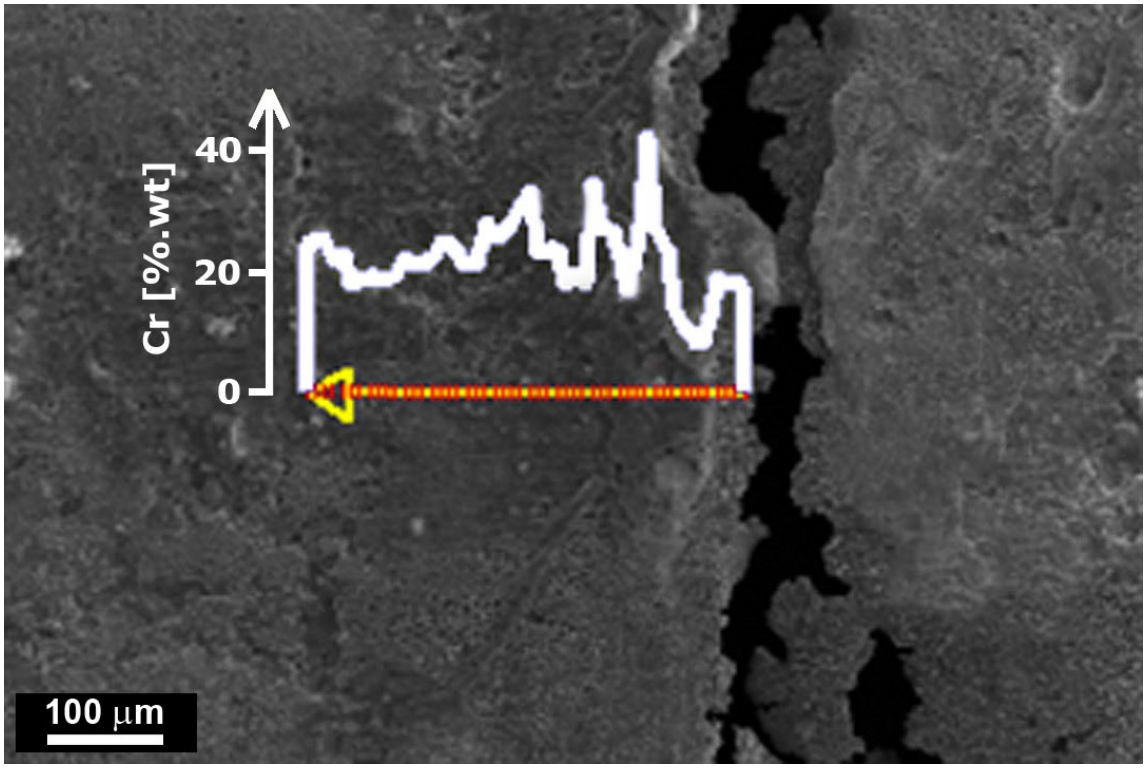

Figure 8 – SEM micrograph of a pit connected into cracks, with an overlaid profile of local variation in chromium concentration, based on the EDX technique. Magnification x200

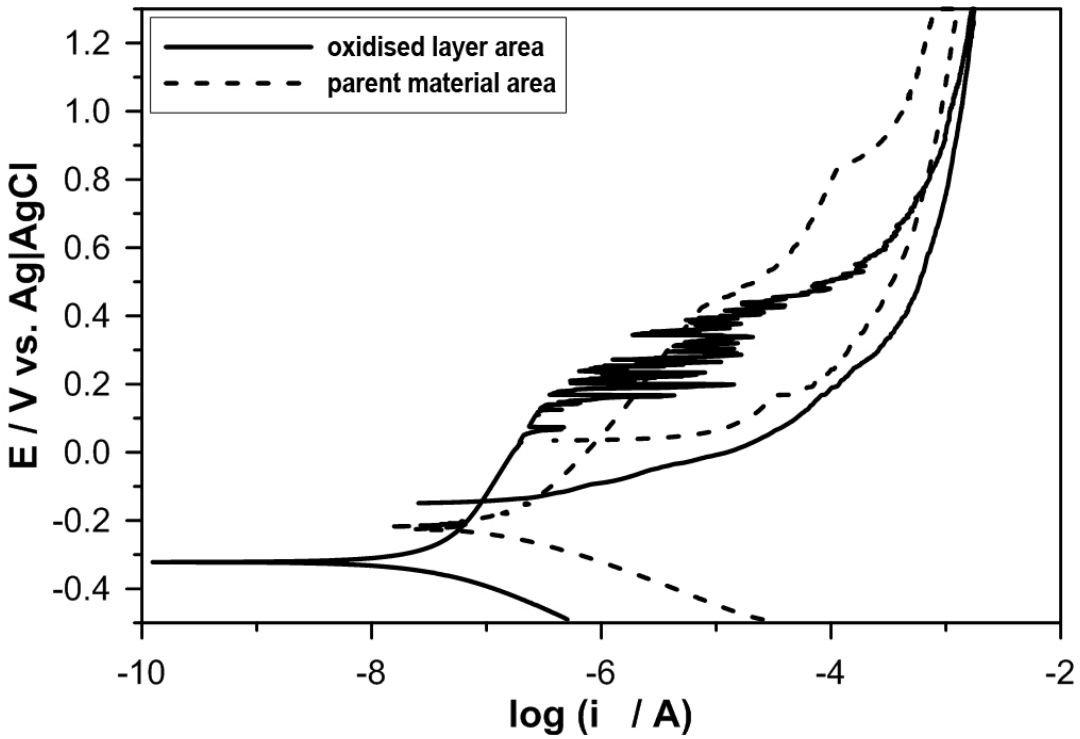

Figure 9 – A polarisation curve for (—) steel AISI 304 in the area of oxidised passive film, and (…) within the area of the parent material.

Table 1 – Analysis of physical and chemical parameters of water

Relevant parameters	Measurement temperature [°C]	22.4
	pH	7.93
	Hardness [mg/dm^{3}CaCO$_3$]	185
	Total alkalinity [mg/dm^{3}CaCO$_3$]	125
	Conductivity [µS/cm]	818
	Dry residue [mg/dm^3]	586
Chemical composition [mg/dm^3]	Oxygen	2.62
	Silica	3.5
	Calcium	46.8
	Magnesium	5.7
	Potassium	4.7
	Nitrates	1.40
	Chlorides	172.99
	Sulphates	59.0
	Phosphates	4.80
	Hydrogen carbonates	152.50

Table 2 – Spectrophotometry of alloying agents in steel for individual elements of pipelines.

Parent material				**Weld**			
Cr	**Ni**	**Mo**	**C**	**Cr**	**Ni**	**Mo**	**C**
18.01	8.10	0.27	0.06	18.75	8.81	0.64	0.07